Energy & Environmental Science

PERSPECTIVE

View Article Online
View Journal | View Issue

Check for updates

Cite this: *Energy Environ. Sci.*, 2019, **12**, 2605

Room-temperature liquid metal and alloy systems for energy storage applications

Xuelin Guo,† Leyuan Zhang,† Yu Ding,† John B. Goodenough and Guihua Yu *

Liquid metals (LM) and alloys that feature inherent deformability, high electronic conductivity, and superior electrochemical properties have attracted considerable research attention, especially in the energy storage research field for both portable devices and grid scale applications. Compared with high temperature LM systems requiring rigorous thermal management and sophisticated cell sealing, room temperature LMs, which can maintain the advantageous features of liquids without external energy input, are emerging as promising alternatives to build advanced energy storage devices. Moreover, compared with high-temperature liquid metal alternatives, RT-LMs are free of thermal management, corrosion, and sealing issues. In this perspective, we summarize recent advances, analyze current challenges, and provide prospects of the RT-LM systems as electrodes for rechargeable batteries. Starting with an introduction of LM systems and their features, we present the status of the development of liquid metal anodes. Theoretical and experimental explorations of mechanisms including phase equilibria, wetting behavior, and alloy deposition behavior in a battery using liquid metal electrodes (LME) are provided to guide the battery design. Taking Na–K alkali metal alloys and Ga-based fusible alloys as two model LME systems, different battery designs are presented along with mechanistic discussions on cathode dependence, interfacial chemistry, and the multi-cation effect. In addition, other possible battery designs, major challenges, and possible opportunities for further developments of the RT LM-based energy storage systems are also discussed in the end.

Received 28th May 2019,
Accepted 28th June 2019

DOI: 10.1039/c9ee01707k

rsc.li/ees

Published on 28 June 2019. Downloaded by Fail Open on 7/23/2025 10:07:25 AM.

Broader context

Satisfying requirements for massive renewable-energy utilization is one of the most urgent missions of the worldwide research community. The major challenges lie in the development of high-performance, environment-friendly, and cost-effective energy storage systems considering the intermittent nature of renewable sources. Traditional lithium ion batteries show limited specific capacity and energy density, while lithium metal batteries that could potentially provide high energy density face a severe dendrite growth problem as an intrinsic feature of alkali anodes. Employment of liquid metal electrodes with self-healing features provides a viable solution to intrinsically address the dendrite issue. Differing from the previously established high-temperature liquid metal batteries (LMBs) that need excess thermal energy to melt the high melting-point metals, fusible alloys that are in the liquid phase at or near room-temperature could considerably help control the energy input and simplify the cell fabrication. Two major RT-electrode systems that have been reported recently, Na–K alloys and Ga-based alloys, are mainly discussed in this perspective. Na–K alkali metal alloys composed of more earth abundant elements could replace Li metal anodes, and Ga-based alloys could work as self-healing high-capacity alkali-ion (Li, Na, *etc.*) anodes.

1. Introduction

1.1 LMB development and key features

Lithium ion batteries (LIBs), one of the most promising energy storage devices, normally adopt insertion-based electrodes for a stable electric source in commercial products. However, the energy and power density of LIBs have yet to be improved to meet the growing demand for widespread applications.[1] High energy lithium metal anodes have attracted the interest of researchers again recently, although they have been condemned due to the dendrite issue and low efficiency problem caused by the inactive solid electrolyte interphase (SEI) and dead lithium formation.[2] Methods for preventing the dendrites from growing have been intensively explored, while most of the strategies would partially sacrifice the specific capacity, by introducing some kinds

Materials Science and Engineering Program and Department of Mechanical Engineering, The University of Texas at Austin, Austin, TX 78712, USA.
E-mail: ghyu@austin.utexas.edu
† These authors contributed equally to this work.

Published on 28 June 2019. Downloaded by Fail Open on 7/23/2025 10:07:25 AM.

of substrates, or cannot essentially solve this problem.[3–8] Besides, utilizing conductive polymer-based electrolytes or substrates in solid-state batteries is another emerging approach to solve these issues.[9,10] However, the poor interfacial contact of the solid-state batteries still remains as a critical challenge. More importantly, it has been reported that with the growing need of lithium, the consumption of the lithium storage on the earth increases exponentially and would reach 1/3 in 2050.[11] Therefore, looking for a suitable alternative for Li in batteries is an urgent task for various concerns.

Liquid metals or alloys, thanks to their fluidity, could intrinsically avoid the dendrite problem while keeping good contact at interfaces compared with solid-state electrodes. The faster mass transport in the liquid phase could potentially help increase the mass transfer kinetics, which makes the LMEs suitable for high power applications.[12] Since the liquid metals have high surface tension and different wettability on various surfaces, it is possible to realize the confinement of the fluidic LM with those properties as well. Many elements that could form liquid metals are more earth abundant than Li (Table 1). It has been widely studied that some molten metals or alloys could work as high capacity electrodes at high temperature.[13] Most of the alloying reaction-based electrode materials could be practical for this design, while extra energy input to melt the metals and specially designed corrosion-resistive battery components at high operating temperature become necessary. Specifically, the commonly adopted liquid metals, especially alkali metals, are very sensitive and reactive under high operating temperature. Therefore, sealing technology becomes one of the most important concerns, since leakage could cause a severe safety problem. What is more, liquid metal cathodes of relatively low potential limit the entire battery energy output to be insufficient for most applications. A Na–S battery working at 300–350 °C using molten sodium and sulfur as active materials and a Zebra-cell with molten Ni/$NiCl_2$ and Na/NaCl at a similar working temperature are two classical examples of high-temperature liquid metal batteries.[14,15] As a typical battery design in recent research, for example, in a lithium–antimony–lead cell, the molten lithium anode and Sb–Pb cathode were separated by a molten salt (LiF–LiCl–LiI) at 253 °C, and the battery has good cyclability for 450 cycles with high coulombic efficiency (CE).[16] However, since the lithiation potential of the alloy cathode adopted to work at a reasonable temperature is relatively low, the total battery voltage only reached less than 0.9 V. These prototype liquid metal batteries are clearly far from practical in real-world applications. To fulfill the requirement of the industry, less energy input (no heating) and more energy output (high voltage) should be achieved.

1.2 Fusible alloys for room-temperature LMBs

Recently, research focus has been transitioned to room-temperature liquid metal electrodes thanks to their superior properties as shown in Fig. 1. There are several recognized fusible metal systems, including mercury metal, alkali metal alloys, Ga-based alloys, and alloys containing only bismuth, lead, tin, cadmium, zinc, indium, *etc.* A mercury dropping electrode (DME) has been one of the perfect choices for spherical electrode characterization tests. Hg-based batteries, *e.g.* Zn–Hg batteries, are also famous first-type or non-rechargeable batteries that have been on the market for years.[19] However, since the redox reaction of Hg has the reversibility issue and Hg is toxic, they are not an ideal choice for secondary battery applications. Fusible alloys, which refers to the group of alloys that have low enough melting temperature to be in the liquid phase around or at a temperature slightly higher than room-temperature (well below 183 °C), are normally composed of metals that have low melting points as well. The commonly studied fusible alloys for battery applications are typically composed of two or more metals that are all alkali metals, or Ga-based high thermal conductivity metals.

Na, K, and Cs alloys, composed of two or three elements, have a strong tendency of alloying and forming eutectics. Since the reduction potential for most of the alkali metals is very low, once a reasonable cathode is matched the battery could run at a

Table 1 Summary of melting temperature (MT) and standard reduction potentials for corresponding reactions at RT for selected low-melting-temperature metals and fusible alloys[17,18]

Metal/alloy	MT (°C)	Name	Reaction	Potential (V)
Hg	−38.8		$Hg^{2+} + 2e \leftrightarrow Hg$	0.8
Cs	28.5		$Cs^{+} + e \leftrightarrow Cs$	−2.92
Ga	29.8		$Ga^{3+} + 3e \leftrightarrow Ga$	−0.52
Rb	39.3		$Rb^{+} + e \leftrightarrow Rb$	−2.98
K	63.5		$K^{+} + e \leftrightarrow K$	−2.92
Na	97.79		$Na^{+} + e \leftrightarrow Na$	−2.71
In	157		$In^{3+} + 3e \leftrightarrow In$	−0.34
Li	180.5		$Li^{+} + e \leftrightarrow Li$	−3.01
Sn	231.9		$Sn^{2+} + 2e \leftrightarrow Sn$	−0.14
Cs73.71, K22.14, Na4.14	−78.2	—		
K76.7, Na23.3	−12.7	—		
Ga88, Sn12	25	—		
Ga62.5, In21.5, Sn16	10.7	Galinstan		
Ga75.5, In24.5	15.7	EGaIn		
Bi44.7, Pb22.6, In19.1, Cd 5.3, Sn8.3	47	Cerrolow 117		
Bi32.5, In51, Sn16.5	60.5	Field's metal		
Sn62.3, Pb37.7	183	Eutectic solder		

 This journal is © The Royal Society of Chemistry 2019

Published on 28 June 2019. Downloaded by Fail Open on 7/23/2025 10:07:25 AM.

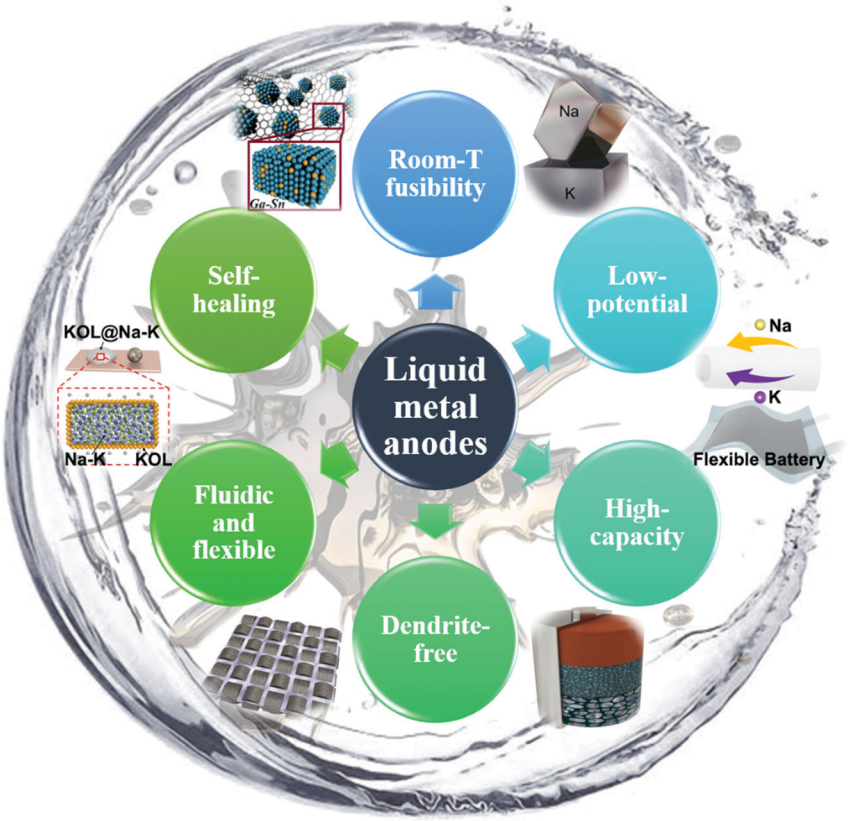

Fig. 1 Schematic illustration of the features and advantages of liquid metal anodes.

decently high voltage. Na–K alloys, as one of the eutectic systems with alkali metal fusible alloys, have been reported as alkali metal anodes recently for battery applications. In this binary system, sodium has a reduction potential of −2.71 V, while potassium has a potential of −2.92 V, both close to lithium (−3.01 V), and have been reported to work as possible anodes.[18] Due to its high surface tension and special wetting behavior, searching for suitable host substrates and understanding its wetting behavior on different substrates for the Na–K alloy became essential.

Ga-Based liquid alloys, on the other hand, are normally less suitable for direct use as metal anodes with themselves being charge carriers as the alkali metals. Firstly, their reduction potentials are typically high, for example gallium, tin and indium have reduction potentials of their +2 or +3 valence states at −0.56 V, −0.14 V and −0.34 V, which could hardly fulfill the requirement for high battery voltage.[18] Secondly, the ionized forms of those metals prefer to be multivalent and have relatively large ionic radius, which makes the electrostatic force significantly hinder those ions from fast transport. However, those alloys are good conversion-type or alloying-type anodes to host Li/Na ions that have high capacity and low potential. The insertion of Li ions into a host alloy, for example, Si anodes, could result in extremely large capacity and their alloying potential is about 0.1–0.8 V for most cases.[20] Compared with the Si anode that has a large volume change and severe delamination problems, the LM alloying-anodes could also be lithiated with high capacity and would change back to the liquid phase once de-lithiated to recover any defect that might have been created during lithiation. In the following, we will introduce the thermodynamic and physical behaviors of liquid metals, battery chemistries and battery designs using fusible LM as anodes, and discuss future opportunities of LM systems in advancing the energy storage field.

2. Mechanistic considerations for LMBs

2.1 Phase equilibria and eutectic

Liquid metal batteries employing LMEs have intrinsic advantages, such as self-healing properties, dendrite-free behavior, fast reaction kinetics and long lifetime.[13,21] Based on the physico-chemical properties, the potential candidates for developing promising LMEs should be electroactive metals with low melting point. In addition to considering the temperature factor, it is also important to evaluate the cost of materials when selecting possible metals for LME designs. As summarized in Table 1, the potential metal candidates with melting point below 200 °C are Hg, Cs, Ga, Rb, K, Na, In, and Li.[21] However, considering their electrochemical activity, melting temperature, cost, and environment amenity, Ga, In, Sn and alkali metals (Li/Na/K) are considered as valuable alternatives for liquid metal based energy storage because they are capable of forming liquid metal alloys at room

Published on 28 June 2019. Downloaded by Fail Open on 7/23/2025 10:07:25 AM.

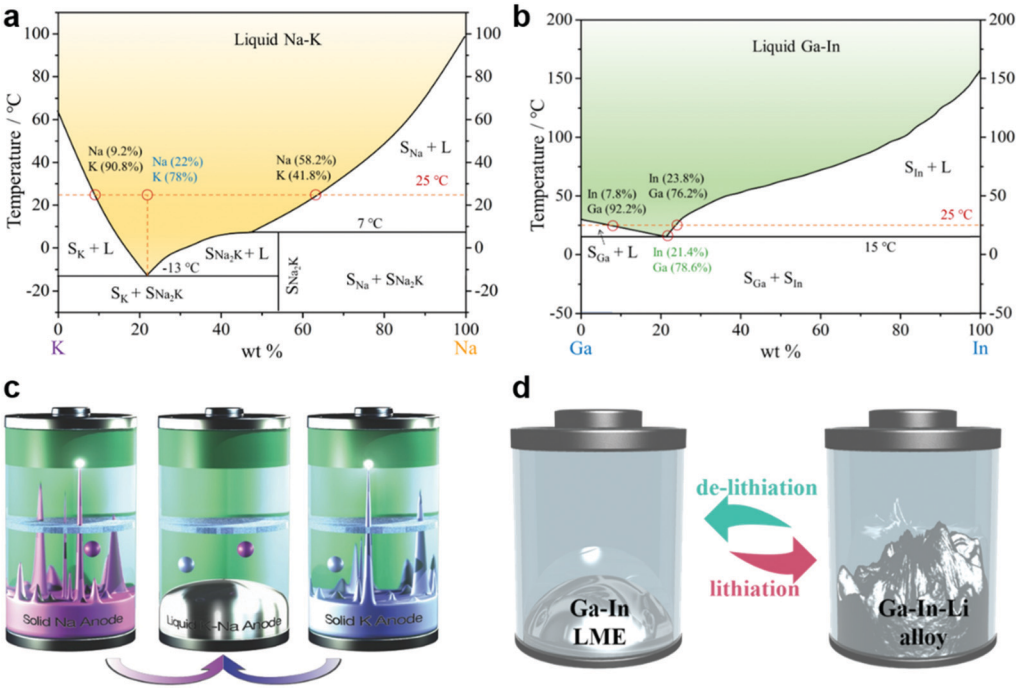

Fig. 2 (a and b) Phase diagrams of a Na–K alloy system and a Ga–In alloy system, respectively. (c) Schematic of a room-temperature Na–K alloy anode in a battery to show the advantage of self-healing properties and dendrite-free behavior. For solid Na or K metals, serious dendrite growth can penetrate through separators to cause internal short-circuit. Reprinted with permission.[22] Copyright 2016 Wiley-VCH. (d) Schematic of the self-healing behavior of the Ga–In alloy as the anode in terms of Li intercalation.

temperature, which is beneficial to avoid the corrosion issue and high maintenance cost in high-temperature LMBs.

To date, two typical kinds of room-temperature liquid metal alloys, Na–K and Ga-based alloys, have attracted much attention for the design of liquid-metal-based energy storage due to their advantageous features of high electrochemical activity and appropriate redox potentials. For Ga-based alloys, several binary and ternary systems are developed to realize the design of LMBs at room temperature, such as Ga–In, Ga–Sn or Ga–In–Sn. As examples, Fig. 2a and b present the phase diagram of Na–K and Ga–In alloy systems, respectively. The Na–K phase diagram has a eutectic point at about −13 °C, which is much lower than room temperature, and it also shows a peritectic line at 7 °C with the existence of a stoichiometric compound, Na_2K(s).[23,24] Actually, there are two small and narrow regions distributed on two sides, respectively, in the reported phase diagram, showing the formation of solid solution. And the solid solution has a body-centered cubic structure consistent with Na or K metal, while the Na_2K compound shows a hexagonal close packed structure. On the other hand, the solid alkali metal anodes (Na or K) would have serious dendrite growth problem during the repeated stripping/deposition process, while the liquid alloy is capable of showing dendrite-free operation and self-healing behavior, as presented in Fig. 2c. However, it is important to maintain the alloy composition in an appropriate region for the design of dendrite-free liquid Na–K electrodes, because the composition experiences a dynamic variation during the electrochemical process with the risk of losing the self-healing property and liquidity. The Na–K system has a specific composition of 22 wt% Na and 78 wt% K at the eutectic point. In order to maintain the liquid state of the Na–K alloy, the composition variation must be confined in a specific region, as identified by the point of intersection on the phase diagram at a temperature level of 25 °C. The specified liquid zone for the Na–K alloy with dendrite-free behavior at room temperature (25 °C) extends from 9.2 to 58.2 wt% Na.

Meanwhile, Ga-based alloys experience different electrochemical processes during charging and discharging compared to the stripping–deposition process of the Na–K liquid alloy. Taking the Ga–In system as an example, it shows a high theoretical capacity for both Li and Na.[25] During the discharging process, Li- or Na-ions could be reduced at the conductive surface and diffuse into the LME to further complete the alloy reaction, leading to a volume expansion (Fig. 2d). And it should be noted that the lithiation or sodiation reaction could cause the phase transformation from liquid to solid which might lead to the fracture or pulverization of electrodes or metal particles. While in the de-lithiation or de-sodiation process, the electrode would be able to transform back into the liquid metal state, eliminating the surface defects or reuniting pulverized particles. Therefore, Ga-based alloys can also be adopted as self-healing and deformable electrodes. Specifically, the Ga–In alloy system has a typical binary phase diagram with a eutectic composition of 21.4 wt% In and 78.6 wt% Ga at 15 °C, which is lower than room temperature.[26] At the intersections of the temperature line at 25 °C, the liquid zone with a range from 7.8 wt% to 23.8 wt% indium content can be determined as the deformable region at room temperature. In addition to the Ga–In system, less expensive

 This journal is © The Royal Society of Chemistry 2019

Published on 28 June 2019. Downloaded by Fail Open on 7/23/2025 10:07:25 AM.

alternatives such as Sn or Al can also be alloyed with Ga to form room-temperature LMEs.

2.2 Liquid metal wetting behavior

Importantly, to drive applications of liquid metals in the energy storage field, fundamental chemistries need to be explored and addressed, such as wetting behavior, conductive substrate effect, interfacial chemistry and so on. In practice, the wetting behavior of liquids on solid substrates has been an important research aspect of surface chemistry for a long time.[27,28] The elementary processes of wetting can be observed in liquid penetration into pores and thin capillary channels of the solid phase and liquid spreading over solid surfaces. In classical theory, the wetting system includes three parts: solid substrate, liquid and gas (pores). The key parameters to evaluate the wettability are the wetting angle (contact angle) (θ) and the surface tension of the liquid (σ_{lv}). Classical wetting theory defines the main thermodynamic relation of surface tension with the wetting angle and the adhesion work (w_a).

$$\cos\theta = \frac{\sigma_{sv} - \sigma_{sl}}{\sigma_{lv}} \quad (1)$$

$$w_a = \sigma_{lv} \times (1 + \cos\theta) \quad (2)$$

where σ_{sv}, σ_{sl} and σ_{lv} are the surface energies at the solid body–gas, solid body–liquid and liquid–gas interfaces.

Eqn (1) and (2) are known as the Young equation and they can lead to two other fundamental equations, known as the Dupre and Young–Dupre equation:

$$w_a = \sigma_{sv} + \sigma_{lv} - \sigma_{sl} \quad (3)$$

$$\cos\theta = \frac{w_a}{\sigma_{lv}} - 1 \quad (4)$$

In addition to conventional non-reactive wetting, the chemical interaction between the liquid and solid body can result in the reactive wetting process, which changes the surface energy (σ_{sl}).[29] The bonding energy of the newly formed chemical bond can be considered as the adhesion work. Thus, if the chemical reaction has a more negative Gibbs free energy, the interfacial tension between the liquid and solid body would be smaller. Moreover, the kinetics of adsorption and spreading of liquid on the solid surface also has an important effect on the wetting behavior.

For the wetting behavior of liquid alkali metals, the most studied example is molten liquid lithium, which can be used as the reference for a general understanding of the wetting behavior of liquid alkali metals. In order to better utilize lithium metal anodes in practical lithium metal batteries, the wetting behavior of molten liquid lithium has attracted increasing interest recently. However, many available conductive substrates cannot be easily wetted by liquid lithium metal. Currently surface modification strategies are mainly used to improve the wetting of lithium.[30]

Recently, a systematic study of the wetting behavior of molten lithium has been reported, presenting a comprehensive understanding of the fundamental mechanism and the effects of temperature, coating thickness, surface topography and oxide layer on the wetting process.[31] In the work, based on the contact angle, the surface of substrates can be divided into two types, lithiophobic ($>90^\circ$) and lithiophilic ($<90^\circ$) states, as shown in Fig. 3a. In a conventional case, when molten lithium contacts a solid substrate, the liquid droplet would tend to retain its ball shape due to the high surface tension. But a coating of Li-reactive materials can facilitate the spreading of liquid lithium and then decrease the contact angle. The driving force for lithium spreading, as demonstrated in the work, is provided by the negative Gibbs free energy released by the

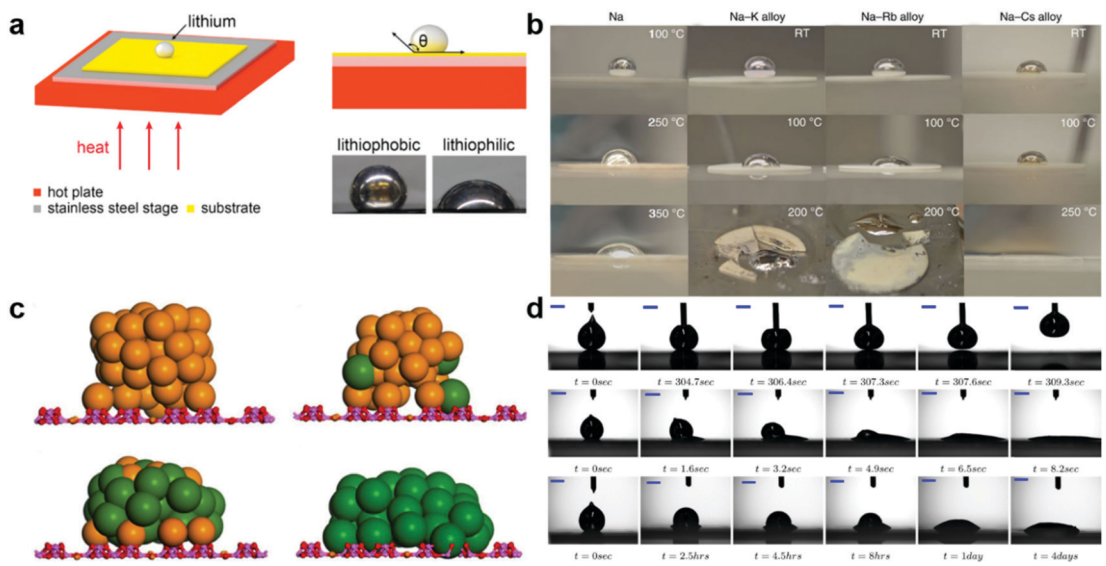

Fig. 3 (a) Schematic of the experimental setup for wettability study and evaluation of contact angle based on molten lithium. Reproduced with permission.[31] Copyright 2018, Elsevier. (b) Wetting behavior of Na and Na alloys on a BASE surface at different temperatures and (c) simulated wetting of liquid Na–Cs alloy droplets on BASE. Reprinted with permission.[32] Copyright 2014 Springer Nature. (d) Wetting behavior of Ga–In and Ga–In–Sn alloys on the surface of sputter coated In or In foil or Sn foil. Reprinted with permission.[33] Copyright 2013 American Chemical Society.

Published on 28 June 2019. Downloaded by Fail Open on 7/23/2025 10:07:25 AM.

reactions between Li and the coating layers on the substrate, among which gold coating has been found to have the lowest energy and best wetting. Furthermore, the coating thickness of Li-reactive materials could also affect the wettability. In addition to the factor of Li-reactive material effect, they also explored the influence of temperature. Contact angles for all the tested substrates decreased when the testing temperature increased, since both the surface tension and viscosity of liquid lithium would be reduced at higher temperatures. On the other hand, although it is important to keep the lithium surface clean for the investigation of wetting behavior, it will be inevitable to have the oxide layer (Li_2O) on the surface of liquid lithium due to the high reactivity, which can generate a kinetic spreading resistance for the wetting of liquid lithium. The reaction between liquid lithium covered by Li_2O layers with Au was also performed to better understand the hindering effect on the spreading of liquid lithium. When the liquid droplet touched Au, the immediate Li–Au reaction caused the break of surficial Li_2O films, resulting in the continuous leaking of fresh liquid along with the spreading on the substrate. In addition to temperature and surface chemistry, the surface topography also has an influence on the wettability, especially for porous substrates. Using Ni foam as an example, the rough surface topography and trapped inert gas could give rise to poor wettability.

Given their similar physicochemical properties, liquid sodium and potassium with lower melting temperature have similar wetting behavior to lithium.[34] Besides the wetting between liquid alkali metals and substrates as current collectors, the wetting of the solid–electrolyte interface is also a common issue for the development of alkali metal batteries. For example, poor sodium wetting is one of the most challenging issues in sodium–beta alumina batteries (Na–S or sodium–metal halide batteries). Even though sodium melts at 98 °C, much higher temperature (400 °C) is usually required to obtain good wetting on the surface of β-Al_2O_3 solid electrolyte (BASE).[35] Similar to the lithium case, the poor wetting of sodium on BASE is believed to be caused by the formation of a surface oxide film, which will hinder the Na-ion transport across the interface. To address this wetting problem, several possible approaches have been demonstrated including surface coating of Pb, Bi or Sn, adoption of oxygen absorbers or use of metal wicks. However, all the mentioned strategies may lose their effect when the operation temperature decreases to 200 °C. The alloying strategy was proposed to improve the wetting of sodium on Na–BASE to enable successful operation at low temperatures (Fig. 3b).[32] The designed Na-based alloys were Na–K, Na–Rb and Na–Cs systems. Since wetting between different surfaces is generally affected by surface energy, the change of the atomic environment in the alloys can change the surface energy and then improve the wetting. As seen in the contact angle experiment, the Na–Cs alloy showed the best wettability on BASE at low temperatures. *Via* simulation of the wetting process (Fig. 3c), it was further confirmed that the wetting gradually improved with the increase of Cs amount in the Na–Cs alloys. Based on the wetting theory, the wettability of liquid metal on the solid surface can be determined by the work of adhesion. And it was calculated that liquid Cs showed a larger work of adhesion and smaller surface tension than liquid Na on the BASE surface, inferring a better wettability. However, for practical use, even though Na–Cs could achieve the best wetting, the use of Cs element significantly increased the material cost. The Na–K alloy with the features of low cost and high abundancy showed similarly improved wetting on the surface of Na–BASE, but the direct contact of the Na–K alloy with Na–BASE could cause the fracture of the solid electrolyte separator because of the ion exchange behavior. Moreover, the liquid sodium or potassium would also cause the cracks of K–BASE or Na–BASE, respectively, when in direct contact with the surface of BASE.[35]

For Ga-based alloy systems, extensive applications in the design of flexible electronics and energy storage also require a deeper understanding of wetting on different substrates or interfaces.[36] The well-studied one is the Ga–In alloy system, which can be used as an applicable reference to further understand the wetting behavior of other Ga-based alloys. In the work reported by Wood *et al.*, the wetting behavior of Ga–In or Ga–In–Sn liquid droplets was studied by the test on silicone-based elastomer substrates with thin metal films (Sn or In; rolled or sputtered).[33] And they found that the surface composition, texture and oxide passivation layer played important roles in wettability. By measuring the contact angle and droplet contact diameter as a function of time using the sessile drop method, the wetting process of Ga–In alloys on selected substrates was evaluated. They summarized three distinct wetting states: (i) poor wetting with high contact angle; (ii) conventional partial wetting and (iii) initial conventional partial wetting along with a subsequent reactive wetting. As displayed in Fig. 3d, the sessile drops in the beginning had a conical shape on the front part, indicating the formation of an oxide layer on the surface. Besides, the Ga–In liquid droplet showed a much better wetting with bare In foil than Sn, but sputtered surfaces with rough micro-textures could repel the wetting. The good wettability on In was ascribed to the grain boundary penetration of Ga–In inducing the reactive wetting, while the metallophobic surface resulted from the gallium-oxide skin on the surface of droplets prevented the possible penetration and reactive wetting. For the Ga–In–Sn system, it only showed a conventional partial wetting on bare In foil due to the lower amount of In, while achieved a reactive wetting with Sn foil because of the presence of 10% Sn. Hence, consistent with the wetting behavior of liquid alkali metals, both chemical composition and surface topography have a big effect on the wettability of substrates, and the oxide layer can play a critical role during the dynamic wetting process.

3. Na–K liquid alkali metal anodes

3.1 Liquid Na–K anode substrate design

Designs of liquid–solid or liquid–liquid anode–electrolyte interfaces have recently emerged, using the concept of LME, to address the dendrite growth and interface contact issues. The same philosophy has been demonstrated before in high-temperature batteries by using molten metals but the high operating temperature (>300 °C)

 This journal is © The Royal Society of Chemistry 2019

Published on 28 June 2019. Downloaded by Fail Open on 7/23/2025 10:07:25 AM.

inherits some other problems such as thermal corrosion, sealing issues or high maintenance cost. Herein, exploring the Na–K liquid alloy as a room-temperature LME provides a great opportunity to develop promising LMBs with dendrite-free anodes at room temperature. The key challenges are conductive matrix design to immobilize the Na–K liquid, interface chemistry, and a fundamental understanding of charge carriers.

Goodenough and coworkers utilized the Na–K eutectic alloy as a dendrite-free anode for potassium-ion energy storage.[22] According to the phase diagram of the Na–K system, it was calculated that the Na–K alloy retained in the liquid regime at 25 °C was able to deliver a high capacity of 629 mA h g^{-1} for Na-ion charge carriers and 579 mA h g^{-1} for K-ion charge carriers. In their work, the alloy composition was determined to be about 33 wt% Na and 67 wt% K because it could allow for both charging and discharging in the initial period without any phase separation. What's more, they found that the high surface tension of the Na–K liquid alloy prevented it from penetrating porous membranes (Celgard® or Glass fiber separator) containing liquid electrolytes, which offered the possibility of energy storage application without considering the potential failure of cross over. And in order to further immobilize the liquid Na–K and improve the electrode fabrication and wetting interface, a porous carbon substrate (carbon paper) was applied to absorb the liquid alloy at a high temperature (420 °C), as shown in Fig. 4a. When paired with an $Na_2MnFe(CN)_6$ host cathode, the room-temperature LMB concept was demonstrated with the Na–K composite anode, conventional carbonate electrolytes with $NaClO_4$ salts and glass-fiber separators. It can be also extended for room-temperature liquid Na–K membrane anodes to other available porous substrates, such as Cu, Al, and Ni membrane foams.[37] For example, the Na–K liquid alloy could be fused into metal foams or carbon paper at room temperature (Fig. 4b), which makes the fabrication of membrane anodes convenient and economical. On the other hand, although both copper and aluminum foils are commonly used as current collectors in battery technologies, porous Al foam might be better to accommodate the use of the Na–K liquid alloy since it does not form any alloy with either Na or K, and it is cost-effective. It's also found that the liquid alloy could stay within the metal foams during bending or contacting with separators, which was identical to carbon paper. A room-temperature rechargeable Na-ion LMB design is demonstrated by using a Na–K–Al membrane anode, a $Na_{2/3}Ni_{1/3}Mn_{2/3}O_2$ cathode and common carbonate electrolytes containing $NaClO_4$.[37]

More research efforts were made on achieving room-temperature Na–K liquid anodes with a carbon matrix *via*

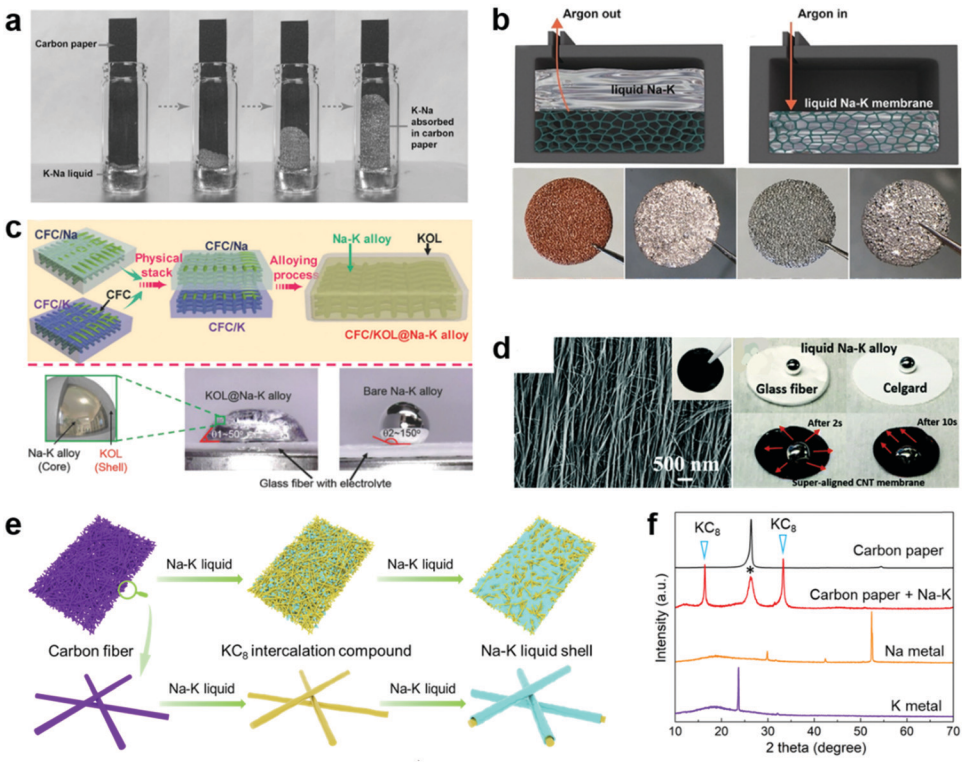

Fig. 4 Fabrication of room-temperature Na–K LMEs using various conductive substrates. (a) The absorption of the Na–K liquid alloy into the carbon paper matrix at 420 °C after immersion in the liquid alloy. Reprinted with permission.[22] Copyright 2016 Wiley-VCH. (b) Vacuum infiltration of the Na–K liquid alloy into various porous substrates (Cu/Al/Ni foams). Reproduced with permission.[37] Copyright 2018 Wiley-VCH. (c) Schematic of the fabrication process of a KOL@Na–K alloy electrode using the CFC matrix under high pressure. Reproduced with permission.[38] Copyright 2018 Wiley-VCH. (d) Fabrication of a Na–K liquid alloy membrane electrode based on super-aligned carbon nanotube membranes. Reprinted with permission.[39] Copyright 2018 Royal Society of Chemistry. (e) Schematic of NaK-G-C electrode preparation to illustrate the formation of the GIC framework (KC_8) at room temperature. Reprinted with permission.[40] Copyright 2019 Royal Society of Chemistry. (f) Characterization of NaK-G-C electrodes. Reprinted with permission.[40] Copyright 2019 Royal Society of Chemistry.

Published on 28 June 2019. Downloaded by Fail Open on 7/23/2025 10:07:25 AM.

tuning the wettability. In Tu's work, they adopted a carbon fiber cloth (CFC) as the conductive matrix to anchor the Na–K liquid alloy.[38] The fabrication involved an *in situ* alloying process: Na and K metals were first pressed into the CFC, separately, and then these two sheets were merged together to induce the alloying reaction between Na and K at room temperature (Fig. 4c). In fact, the Na–K alloy could not wet the CFC at room temperature, and similarly, the CFC/Na–K anode fabrication could be realized only at an increased temperature (400 °C). It's found that the solid K_2O layer (KOL) shell covering the surface of the Na–K alloy could protect the inner Na–K liquid from the attack of liquid electrolytes. The formation of KOL was ascribed to the reaction between trace O_2 in the glovebox and more reactive K with the aid of heat energy released from the alloying process. However, the KOL could be decomposed and removed at a temperature of 380 °C or above. Yang and coworkers reported that the carbon nanotube membrane (CM) woven by super-aligned carbon nanotubes could show a strong affinity to the Na–K liquid alloy (Fig. 4d) and the excellent wettability was due to the strong capillary force resulting from the aligned superstructure.[39] In contrast, if the carbon nanotube membrane was prepared by vacuum filtration with a randomly distributed structure, it would show poor wettability, implying the importance of the aligned texture for the wetting of the Na–K alloy. In their case, the fabricated membrane electrode retained the good flexibility of CM and the surface color changed from black to shiny silver (front) or gold (opposite side), demonstrating the infiltration of the Na–K alloy. Therefore, it is important to note that the capillary force is a crucial factor for LM wettability in design of textured substrates.

Recently, Yu and coworkers reported a facile and scalable synthesis of Na–K composite anodes at room temperature *via* the interaction between the Na–K alloy and carbon matrix without the need for high pressure or a vacuum procedure.[40] As presented in Fig. 4e, it's found that the simple immersion of carbon paper in the Na–K liquid alloy could trigger the diffusion and intercalation of potassium along the carbon fibers inside the carbon matrix. Intriguingly, potassium diffused much faster than sodium, resulting in the formation of a graphite intercalation compound (GIC, KC_8) framework, which could improve the wettability and thus induce the infusion of the Na–K alloy, finally forming a homogeneous room-temperature LME (Fig. 4f). The three major stages of the change in electrode color, blue, gold and shiny states, imply the degree of intercalation of K into the graphitic structure of carbon fibers that correspond to KC_{24}, KC_8 and Na–K alloy. This study also promotes a fundamental understanding of the interface chemistry of Na–K/carbon interactions, particularly the intercalation of K into graphitic carbon structures.[41] Further, they proposed two distinct advantages of their NaK-GIC-carbon (NaK-G-C) electrodes: (i) it was possible to mitigate dendrite growth and retain the integrity of the SEI layer due to the self-healing and deformable properties; (ii) the *in situ* formed GIC framework could facilitate electron conduction and mass transport in the whole matrix. To demonstrate these appealing features, the symmetric cells were assembled, which exhibited a stable electrodeposition continuously for over 5000 h at a high current density of 20 mA cm^{-2}. Even at an extremely high current density of 80 mA cm^{-2}, with an applied capacity of 16 mA h cm^{-2}, the designed Na–K LME was capable to stably deliver a cycle life of 1200 h. In their work, they also claimed the formation of a robust interface with fluoride species in common KFSI-carbonate electrolytes. Finally, versatile alkali metal batteries were developed based on the designed Na–K LME, demonstrating the potential in practical applications. Since the intercalation process of LM into carbon paper was observed experimentally based on the color change, further explorations of more accurate content and loading control in the future would help in better refining the anode preparation technique.

3.2 Cathode dependence and working mechanism of the liquid Na–K anode

Apart from the fabrication of Na–K LME, the working mechanism of Na–K alloy anodes is also attracting increasing attention because the existence of both Na and K will bring up a question: when using Na–K alloy as the anode, which one, Na^+ or K^+ ion, will act as the dominant charge carrier? In a recent work by Goodenough and coworkers, the phenomenon of cathode dependence of Na–K alloy anodes was observed for the first time.[42] If the applied cathode materials could only allow the insertion of Na^+ ions, such as the layered $Na_{2/3}Ni_{1/3}Mn_{2/3}O_2$ or NASICON-structured $Na_3V_2(PO_4)_3$, the Na–K liquid alloy would only act as a Na anode, using Na^+ ions as the charge carrier. However, when the applied cathode material was $MnFe(CN)_6$, which had a large octahedral interstitial space to host both Na^+ and K^+ ions, $Na_2MnFe(CN)_6$ transformed into $K_2MnFe(CN)_6$ after a few cycles when coupled with Na–K alloy anodes in the initial $NaClO_4$-carbonate electrolytes (Fig. 5a). Meanwhile, the working ion changed from Na^+ to K^+ during the cycling. This transformation procedure could be clearly monitored by the voltage evolution with cycling, as shown in Fig. 5b. In addition, when $KClO_4$ was used as the initial electrolyte salt, the $Na_2MnFe(CN)_6$ cathode would quickly transform into $K_2MnFe(CN)_6$. Thus, they proposed the conclusions: (i) the determinant of whether the liquid Na–K is a Na or a K anode is the energy gained by insertion of K^+ *versus* Na^+; (ii) if the cathode host cannot accept K^+ ions, it acts as a Na anode; (iii) if both Na^+ and K^+ can be inserted into the cathode, and the cathode host prefers K^+ over Na^+, it acts as a K anode.

In another recent work by Yu and coworkers, sodium rhodizonate dibasic (SR) was explored as an organic cathode that showed negligible preference toward Na^+ and K^+ ions to prove that liquid electrolytes played an important role in determining the working ions because of the selective ion path controlled by the SEI.[43,44] As mentioned previously, although K metal has a lower redox potential than Na metal, many other factors should also be considered to fully understand the working mechanism. For example, compared to conventional inorganic intercalation cathode materials, organic materials have unique advantages in terms of elemental abundance, molecular diversity and cation storage selectivity. Thus, by combining the advantages of Na–K alloy anodes with organic cathode materials, it opens great opportunities to develop flexible and sustainable energy storage

 This journal is © The Royal Society of Chemistry 2019

Published on 28 June 2019. Downloaded by Fail Open on 7/23/2025 10:07:25 AM.

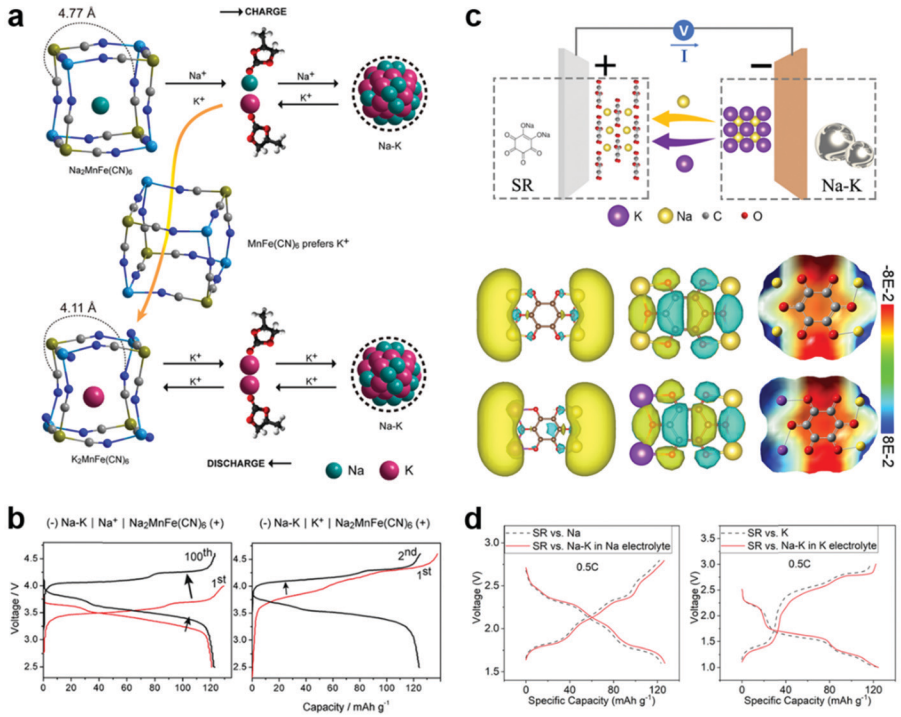

Fig. 5 Cathode-dependent behavior of the Na–K liquid alloy anode. (a) When working with a $MnFe(CN)_6$-based cathode material, the Na–K liquid alloy anode acts as a potassium anode and (b) corresponding galvanostatic curves. Reproduced with permission.[42] Copyright 2018, American Chemical Society. (c) Schematic of SR insertion mechanism showing no energy preference towards Na and K ions based on DFT calculations and (d) corresponding voltage profiles of SR/Na–K batteries in Na-ion or K-ion electrolytes. Reprinted with permission.[43] Copyright 2019 Wiley-VCH.

devices. As displayed in Fig. 5c, density functional theory (DFT) calculations on the energy of different reaction products confirmed that the SR cathode host could accommodate both Na^+ and K^+ ions without the obvious difference in terms of potential and charge distribution. Then they further conducted electrochemical charging and discharging to verify the proposed concept by employing different electrolytes in the constructed SR/Na–K coin cells (Fig. 5d). By comparing the voltage profiles including potential plateaus, capacity and overpotentials, the constructed batteries with either Na–K or Na/K anodes almost showed identical charging and discharging curves in the same electrolytes, indicating the electrolyte-dependent behavior. And they further conducted multiple characterizations including XRD and XPS techniques to confirm the role of the SEI layer in the regulation of the working mechanism of Na–K anodes. Based on all these measurements, it was proposed that the formed SEI in different electrolytes functioned as an ionic pathway that governed the working mechanism of the Na–K alloy under the condition that cathode materials did not have a preference toward alkali cations. Besides, benefiting from the potential flexibility of both LME and organic cathode, a flexible battery was demonstrated with an ultrahigh areal capacity and the same concept could also be extended to other promising organic cathode materials.

4. Ga-Based alkali ion liquid metal anodes

Gallium-based fusible alloys, especially EGaIn, have been widely reported as promising liquid metals for semiconductors in electronic applications, due to their fluidity that could fulfill the requirements of flexible and self-healing electronics. For example, Markvicka and coworkers have reported a soft robotics design based on EGaIn, which has EGaIn circuit components on a flexible elastomer substrate as the sensor, and it could recover the connection after damage.[45] Since the liquid has different wetting properties, one could control the shape and position of a LM droplet with an applied potential.[46] In the field of batteries, the Ga-based alloys are also good choices because of their high capacity of alkali ion storage. Based on the phase diagram, the composition that has the highest alkali ion concentration indicates the highest form of alloy that is thermodynamically stable, which is also the highest capacity that the alloy is capable of exhibiting, when the third component is not completely miscible. For example, Ga could form alloys with the highest Li concentration as Li_2Ga, corresponding to a capacity of 768.8 mA h g^{-1}, and the highest Na concentration form as $Na_{22}Ga_{39}$, corresponding to 216.8 mA h g^{-1}. Ga itself has a low enough melting point at around 40 °C, that could work as an LM anode with slight heating. Deshpande *et al.* have reported the direct use of Ga as a LIB anode, with the capacity contributed by each stage of alloying that yields 91% of the theoretical capacity in their electrochemical tests as shown in Fig. 6a.[47] The morphology of the Ga anodes clearly shows the recovery of the cracks after de-lithiation, which indicates the successful self-healing process, and the good rate performance also shows the advantage of the LM anode. However, the cyclability of the cell in this work is limited to less than

Published on 28 June 2019. Downloaded by Fail Open on 7/23/2025 10:07:25 AM.

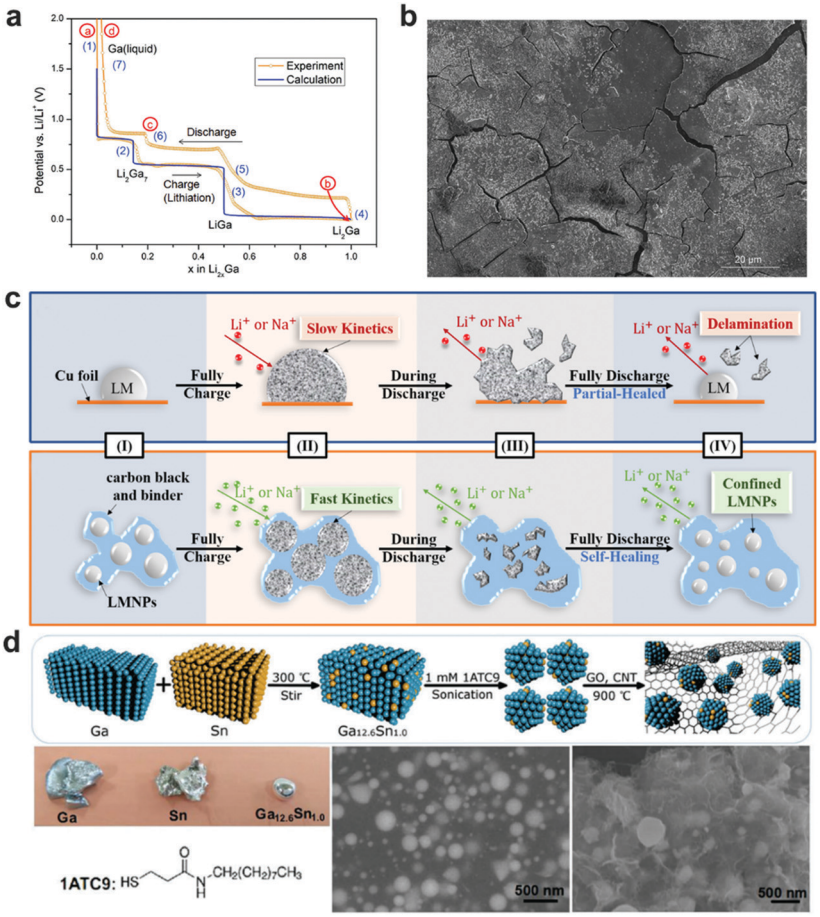

Fig. 6 Ga-Based liquid metal anodes. (a) Cyclic voltammetry (CV) of using Ga as an anode at 40 °C for the self-healing property. Reprinted with permission.[47] Copyright 2011, Electrochemical Society. (b) The surface of the solidified Ga electrode after lithiation. Reprinted with permission.[47] Copyright 2011, Electrochemical Society. (c) Ga–In alloy nanoparticles suspended in conductive carbon and a binder for electrodes as LIB/SIB anodes. Reprinted with permission.[25] Copyright 2018, Royal Society of Chemistry. (d) Ga–Sn alloy with the CNT framework for a Li-ion anode. Reprinted with permission.[48] Copyright 2017, Wiley-VCH.

30 cycles, and the capacity decreases to less than 500 mA h g^{-1} in the first 10 cycles. This shows that not only is extra thermal energy input required, but cracks are also created at the intermediate stage as shown in Fig. 6b. Although the subsequent de-lithiation step could heal the surface, such big cracks could have caused a loss of stability.

For the alloy electrode that is composed of two elements, its working mechanism is normally regarded as the conversion reaction with Li, converting the alloy into a lithium alloy and an elementary substance, and the elementary product is further alloyed with Li to form another alloy, based on the order of reaction potential. For example, if the EGaIn alloy that has 78.2 wt% of Ga is being reacted with Li ions, the system will eventually evolve into a combination of Li_2Ga that has a capacity of 768.8 mA h g^{-1} and $Li_{13}In_3$ with a capacity of 1011.4 mA h g^{-1}, and cooperatively give a capacity of 821.7 mA h g^{-1} after being normalized. Yu and coworkers have used EGaIn as the liquid metal anode, that yields a capacity of up to 706 mA h g^{-1} towards Li, and 222 mA h g^{-1} towards Na with the theoretical capacity being 271 mA h g^{-1}.[25] By simply preparing the anode with hundreds of nanometer sized LM nanoparticles (LMNPs) dispersed in carbon black and a binder, as shown in Fig. 6c, the cyclability could be largely improved to at least 500 cycles. Another fusible alloy system, Ga–Sn alloy, has also been reported to be the liquid metal anode. The Chen group dispersed Ga–Sn alloy particles in a graphene oxide (GO) and carbon nanotube (CNT) framework with high temperature (900 °C) treatment as shown in Fig. 6d, and superior cyclability was obtained towards Li ions up to 4000 cycles at 4C.[48] Those works show that extra heating is not necessary to obtain a stable Ga-based self-healing liquid metal anode. By synthesizing the LM into LMNPs, the volume expansion problem could be eliminated, and the kinetics is benefited, leading to much better cycling and rate performance.

In summary, the solidification of Ga-based LM electrodes could be an issue that may cause delamination or cracks, while properly preparing them into particles dispersed in a conductive framework could help in effectively solving the problem. And it has not been considered as a problem for Na–K anodes because of the good conductivity and high tendency of the alloy.

 This journal is © The Royal Society of Chemistry 2019

Published on 28 June 2019. Downloaded by Fail Open on 7/23/2025 10:07:25 AM.

5. Large-scale, hybrid, and other novel designs

5.1 Large scale energy storage application of Na–K alloys

In addition to the application in conventional battery technologies, several attempts of employing Na–K liquid alloys in large-scale energy storage including alkali metal–oxygen batteries or hybrid flow batteries have also been reported recently. Using the Na–K alloy as the LME, Kang and coworkers explored a dendrite-free K–O_2 battery at room temperature (Fig. 7a).[49] In their design, the flowable Na–K alloy was fixed to the bottom of a hollow cylinder, and a K^+ conductive Nafion membrane was used as the separator to avoid the possible reaction between Na–K and O_2. Besides, the Nafion membrane was also sandwiched by two glass fiber membranes absorbed with liquid electrolytes, which could further protect the Na–K alloy from O_2 attacks and improve the wetting among different interfaces. In the electrochemical process, the dominant discharge product was characterized to be KO_2 accompanied by a small amount of KOH, implying that the Na–K alloy acted as a potassium anode. However, although the formation of NaO_2 at the cathode was also thermodynamically feasible, the final product in the Na–O_2 battery using the Na–K alloy anode would transform to be KO_2 due to the stronger reducibility of K and thermodynamically more favorable KO_2 formation, which also verified the cathode-dependent behavior of the Na–K alloy in energy storage applications.

Another example of potential implementation of Na–K in large-scale energy storage is a redox flow battery (RFB). RFB systems, in general, could be applied to grid scale applications with flowable electrolytes, and studies using deep eutectic solvent (DES) systems have been reported employing a similar eutectic phase to liquid metals.[53–56] By coupling the Na–K anode with liquid catholytes, the hybrid flow battery (HFB) design can significantly increase the working voltage, thus achieving a high energy density. Compared to the concept of HFB based on solid alkali metals (Li, Na and K), the advantages of the Na–K liquid alloy are self-healing properties, dendrite-free behavior and potentially high current capability. Rugolo's group proposed a design of versatile high-power HFBs based on the result that the Na–K alloy could have a good wetting with K-β″-alumina at room temperature.[50] Acting as a robust K-ion selective separator, K-β″-alumina enabled the design of K-based HFBs when employing different aqueous or nonaqueous catholytes (Fig. 7b). Three representative catholytes ($K_3Fe(CN)_6$, ferrocene and Br_2) were selected to show a high working voltage of over 3 V. Despite the limited conductivity of K-β″-alumina, the prototype battery could still show a promising maximum power density of 65 mW cm^{-2} at room temperature and >100 mW cm^{-2} at 57 °C, benefitting from the high current capability and low potential of Na–K.

5.2 Supercapacitors and hybrid-cation batteries

LM anodes, due to the fast mass transport kinetics of the alloying process in liquid, and the lower overpotential in the stripping–deposition processes verified by symmetric cells, could allow faster transport of charge carriers across the electrode–electrolyte interface, matching with the fast surface capacitive or pseudocapacitive reactions of supercapacitors.[22,43] Hybrid ion supercapacitors have emerged recently with alkali-cation-based anodes and anion-absorption-based cathodes for stable cycling and high capacity. Alkali metal anodes normally have a very low reduction potential, and when paired with absorption-based capacitive cathodes, the battery voltage could

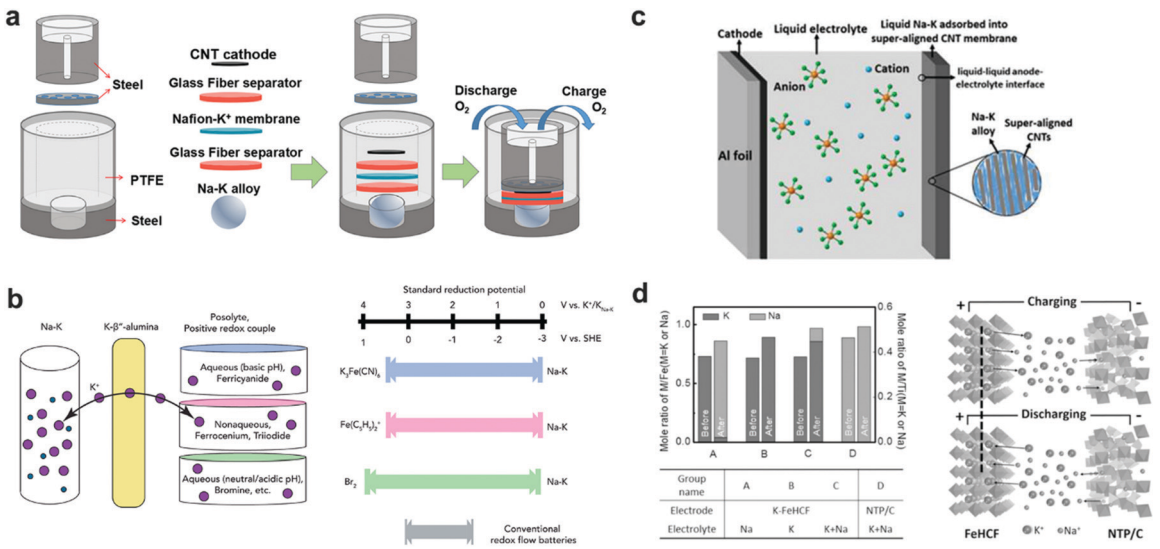

Fig. 7 (a) Schematic of a K–O_2 battery design with the use of Na–K liquid alloy as the anode. Reproduced with permission.[49] Copyright 2017, American Chemical Society. (b) Schematic of a room-temperature Na–K alloy-based hybrid flow battery with various catholyte selections and voltage comparison with conventional redox flow batteries. Reprinted with permission.[50] Copyright 2018, Elsevier. (c) Schematic of a cell anode with alloy liquid adsorbed in CM. Reprinted with permission.[51] Copyright 2018, Royal Society of Chemistry. (d) Schematic of the K–Na hybrid aqueous battery. Reprinted with permission.[52] Copyright 2018, Wiley-VCH.

Published on 28 June 2019. Downloaded by Fail Open on 7/23/2025 10:07:25 AM.

be charged up to as high as the applied electrolyte stability allows. It has been reported that the ClO_4^-, $TFSI^-$, and PF_6^- ions are able to be reversibly absorbed onto the substrate to contribute to the cathodic capacity.[57] An ultrafast supercapacitor with sodium ion insertion on the soft carbon anode and PF_6^- on the hard carbon cathode has been reported to have a capacity of 150 mA h g^{-1} for above 1000 cycles delivering an energy density of 245.7 Wh kg^{-1} at a power density of 1626 W kg^{-1}.[58] Potassium ion and $TFSI^-$ ions with soft carbon on the anode and activated carbon on the cathode have also been reported to have a discharge capacity of 350 mA h g^{-1} for over 1400 cycles.[59] Those works clearly show that with this design, the cathode selection of cations could be avoided, and Na/K cations that normally have a low capacity in most of the insertion-based cathode materials would only work in the anode and therefore avoid affecting the cathode capacity. Therefore, it could be an ideal solution to match the high capacity Na–K alloy anode. Qin *et al.* have reported a RT-liquid-metal-based supercapacitor design with a super-aligned Na–K carbon nanotube membrane as the anode, using activated carbon as the cathode as shown in Fig. 7c.[51] Potassium ion stripping–deposition on the anode side and supporting salt anion absorption on the cathode side collaboratively contributed a capacity of 63 mA h g^{-1} for stable cycling up to 6000 cycles at 2.4 A g^{-1} as well as 41 Wh kg^{-1} energy at 13.3 kW kg^{-1} power. Although the capacity is limited, the stable cycling and high rate performance show the promising stability and fast kinetics of this battery design. More works on matching a suitable high capacity capacitive cathode could help the development of this type of design.

Another type of design for the LM alloy anode is the hybrid-cation battery type. A hybrid-cation battery is specified as a type of battery that has different cations inserted or deposited on different sides of the electrodes. It was reported for a Mg–Li system that the Mg anode is paired with a Li ion insertion cathode to construct the hybrid-cation battery.[60,61] Mg as a well-known metal that has no dendrite problem during the stripping–deposition process is hardly practical in organic metal ion batteries because of the dense oxide layer and limited cathode insertion capability. Similarly, for the Na–K alloy, the Na or K ions normally do not have as much capacity in cathode materials as Li ions, while the dendrite-free behaviour is attractive as an ideal anode candidate. It was reported that similar hybrid-ion batteries could be achieved for the Na–Li system, using a $Na_3V_2(PO_4)_2O_2F$ (NVPOF) cathode for Na-ions and a graphite anode for Li ions that could deliver a high voltage of 4 V and a capacity of 113 mA h g^{-1} for stable cycling over 2000 cycles.[62] A rock-chair type battery with a $K_2FeFe(CN)_6$ K ion cathode and a $NaTi_2(PO_4)_3$/carbon Na anode with the design shown in Fig. 7d also shows stable cycling with 94% capacity retention for 1000 cycles, although the capacity and voltage are limited.[52] However, since Na and K have only a potential difference of 0.2 V, at higher rate and modified electrolyte, stable stripping–deposition of the selected species is an important consideration. Also, if Li ions are introduced into the system, preventing Li deposition on the anode side should be a consideration as well, since Li alloyed into the anode side will destroy the eutectic.

5.3 Other novel device designs and limitations of LMEs

The unique features of the liquid metal allow the possibility of their applications in various energy storage applications. All-liquid metal batteries with both anode and cathode being fusible alloys are a possible battery design, which could ideally be applied in the form of flow batteries with both sides being fluidic components. However, properly matching the cathode and anode alloys to obtain a reasonably high voltage would be a problem. Besides, the superior flexibility of the LM would allow its application in batteries specified for flexible devices. A flexible battery design with a Na–K anode and an organic cathode has been reported by Yu *et al.*, and could be extended to many other cathodes that can be prepared in the flexible state.[43] Recently, the EGaIn alloy has been reported to be printable with 3D printers, which made 3D printed integrated flexible electronic devices possible to obtain flexible batteries as well.[63] With this design, the compatibility of the battery components with the electronic system and safety considerations should be the major issues. Other designs taking advantage of the special wetting and immiscibility of the LMs, like membrane-free batteries, to improve the transportation efficiency are also worth studying.

Although LMEs are gifted with many superior mechanical and electrochemical properties compared with solid metal electrodes, there are still some limitations that need to be resolved at the current stage. For example, the summarized RT-LMs here are mostly limited in a concentration range, which could lead to solidification of LMEs when the extraction or insertion of one component is in excess of the liquid phase region and therefore loss of the advantages. Looking for strategies to utilize the alloy components in a controlled ratio could be a potential solution. Besides, since liquid metals have high surface tension and special wetting behaviors, to better serve as a battery component, more explorations of the contact and wetting of the LMEs with other components, especially liquid and solid electrolytes are necessary. More explorations on a deeper understanding of the mechanism and better approaches to overcome the problems are needed to enable wide applications of LMEs.

6. Summary and prospect

In summary, as depicted in Fig. 8, room-temperature liquid metal and alloy systems are promising anode candidates for energy storage technologies. Due to the fluidic and deformable feature of liquid metals, the LM anodes are intrinsically dendrite-free or have self-healing properties compared with solid state electrodes. The commonly acknowledged Na–K and Ga-based fusible alloys could provide low reduction potential for high battery voltage as well as high capacity and energy density, and the fast mass/charge transport in the liquid anodes would help obtain high power. Compared with high-temperature liquid metal

 This journal is © The Royal Society of Chemistry 2019

Published on 28 June 2019. Downloaded by Fail Open on 7/23/2025 10:07:25 AM.

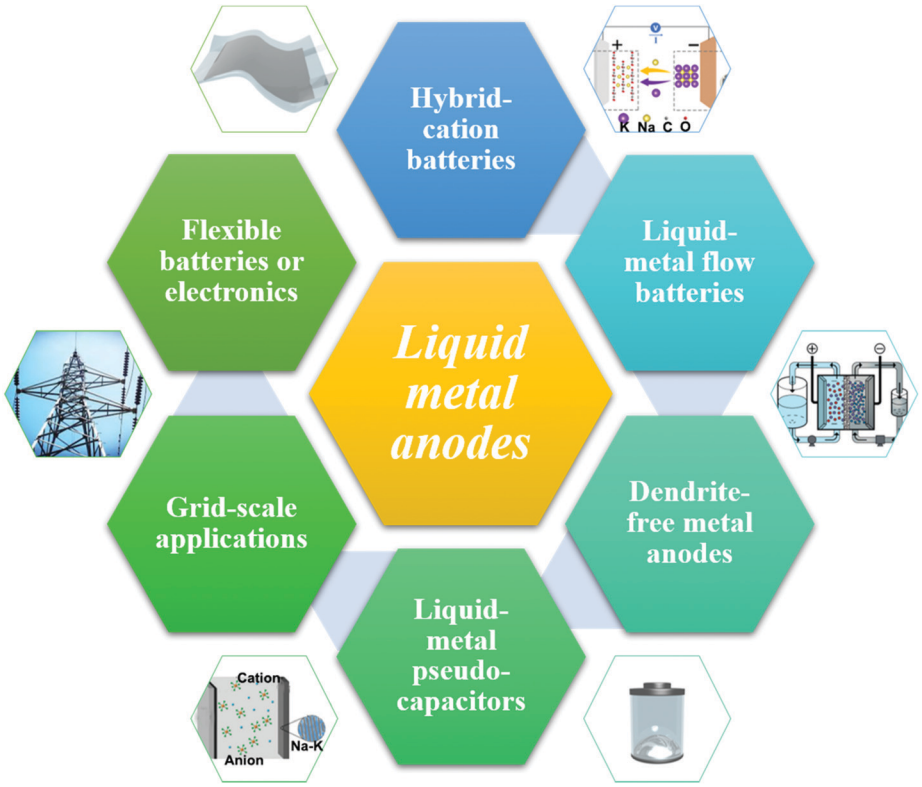

Fig. 8 Prospective designs and applications of the liquid-metal-based electrodes in various energy storage strategies.

anodes, fusible alloys do not need extra energy input to maintain the molten state, which largely controls the cost, improves the energy transfer efficiency, diminishes the possibility of corrosion that might be caused by high temperature, and increases the safety of batteries. The unique wetting behavior of the liquid metal that differs in the presence or absence of an oxidation layer and conversion reaction inducement help us to design the substrate. The flexibility and fluidity of the liquid metal could also allow applications of the LM anodes in flexible batteries and stationary flow batteries. By designing different types of batteries, such as alkali-alloy-based batteries (Na–K), Ga-alloy-based alkali ion batteries, supercapacitors, and hybrid-cation batteries, the LM anode-based anodes could fulfill various requirements in different applications.

Although some encouraging works have been published along this line of research, there are still significant efforts needed to promote potential practical applications. Some of the major tasks are listed as follows:

1. Although the Na–K alloy could help avoid the dendrite-growth problem, it is even more dangerous to expose it to air or moisture than Li due to its higher chemical activity.[64] In particular, when pairing the Na–K alloy with aqueous catholytes, such a HFB design may give rise to potential safety issues, and robust battery packaging with stable membranes and enclosures is still necessary to realize practical applications. Design for safe operations of batteries that could prevent explosion or fire caused by possible leakage is also necessary.

2. For Na–K based anodes, more studies need to be focused on how to quantitatively control the stripping–deposition of one species to prevent the system from being gradually out of the eutectic concentration and solidifying during cycling.

3. For Ga-based anodes, major efforts should be focused on further improving the cyclability, coulombic efficiency, and the reversibility, without sacrificing much volumetric density and capacity.

4. Although the abundancy of K and Ga-based materials is not a problem, the cost is still higher than it should be for some of the species. The metallurgical processing techniques should still be improved for cost-effective production.

5. The species of fusible alloys are limited. To further control the cost and explore other possibilities of liquid metal systems, further understanding and exploration of eutectic alloy systems including Bi–Pb-based LM alternatives is anticipated.

6. The multi-ion system increases the complexity of the battery chemistry. Although the cathode selection mechanism and SEI control mechanism have been proposed, more studies should be carried out to confirm the proposed mechanisms with direct experimental and calculation evidence. Advanced characterization methods and more accurate calculation models should be provided to elucidate more clear mechanisms to guide the battery design for using cathodes with higher capacity and for electrolyte selection.

Conflicts of interest

The authors declare no competing financial interests.

Published on 28 June 2019. Downloaded by Fail Open on 7/23/2025 10:07:25 AM.

Acknowledgements

G. Y. acknowledges financial support from Exxon Mobil Corp, Welch Foundation grant F-1861, and Sloan Research Fellowship. J. G. acknowledges financial support from Welch Foundation grant F-1781.

Notes and references

1 D. Lin, Y. Liu and Y. Cui, *Nat. Nanotechnol.*, 2017, **12**, 194–206.
2 C. Fang, X. Wang and Y. S. Meng, *Trends Chem.*, 2019, **1**, 152–158.
3 C. P. Yang, Y. X. Yin, S. F. Zhang, N. W. Li and Y. G. Guo, *Nat. Commun.*, 2015, **6**, 8058.
4 N. W. Li, Y. X. Yin, C. P. Yang and Y. G. Guo, *Adv. Mater.*, 2016, **28**, 1853–1858.
5 J. Bae, Y. Li, J. Zhang, X. Zhou, F. Zhao, Y. Shi, J. B. Goodenough and G. Yu, *Angew. Chem., Int. Ed.*, 2018, **57**, 2096–2100.
6 R. Zhang, X. B. Cheng, C. Z. Zhao, H. J. Peng, J. L. Shi, J. Q. Huang, J. Wang, F. Wei and Q. Zhang, *Adv. Mater.*, 2016, **28**, 2155–2162.
7 I. H. Son, J. H. Park, S. Park, K. Park, S. Han, J. Shin, S. G. Doo, Y. Hwang, H. Chang and J. W. Choi, *Nat. Commun.*, 2017, **8**, 1561.
8 J. Bae, Y. Li, F. Zhao, X. Zhou, Y. Ding and G. Yu, *Energy Storage Mater.*, 2018, **15**, 46–52.
9 F. Zhao, J. Bae, X. Zhou, Y. Guo and G. Yu, *Adv. Mater.*, 2018, **30**, 1801796.
10 Y. Guo, J. Bae, F. Zhao and G. Yu, *Trends Chem.*, 2019, **1**, 335–348.
11 S. Yang, F. Zhang, H. Ding, P. He and H. Zhou, *Joule*, 2018, **2**, 1648–1651.
12 E. Dologlou, *Glass Phys. Chem.*, 2010, **36**, 570–574.
13 H. Kim, D. A. Boysen, J. M. Newhouse, B. L. Spatocco, B. Chung, P. J. Burke, D. J. Bradwell, K. Jiang, A. A. Tomaszowska, K. Wang, W. Wei, L. A. Ortiz, S. A. Barriga, S. M. Poizeau and D. R. Sadoway, *Chem. Rev.*, 2013, **113**, 2075–2099.
14 Z. Wen, Y. Hu, X. Wu, J. Han and Z. Gu, *Adv. Funct. Mater.*, 2013, **23**, 1005–1018.
15 G. Li, X. Lu, J. Y. Kim, K. D. Meinhardt, H. J. Chang, N. L. Canfield and V. L. Sprenkle, *Nat. Commun.*, 2016, **7**, 10683.
16 K. Wang, K. Jiang, B. Chung, T. Ouchi, P. J. Burke, D. A. Boysen, D. J. Bradwell, H. Kim, U. Muecke and D. R. Sadoway, *Nature*, 2014, **514**, 348–350.
17 R. W. Ohse, *Handbook of thermodynamic and transport properties of alkali metals*, International Union of Pure and Applied Physics, United Kingdom, 1985.
18 A. J. Bard and L. R. Faulkner, *Electrochemical Methods: Fundamentals and Applications Second Edition*, Wiley, 2001.
19 A. J. Salkind and S. Ruben, Mercury Batteries for Pacemakers and Other Implantable Devices, in *Batteries for Implantable Biomedical Devices*, ed. B. B. Owens, 1986.
20 C. Wang, H. Wu, Z. Chen, M. T. McDowell, Y. Cui and Z. Bao, *Nat. Chem.*, 2013, **5**, 1042–1048.
21 H. Li, H. Yin, K. Wang, S. Cheng, K. Jiang and D. R. Sadoway, *Adv. Energy Mater.*, 2016, **6**, 1600483.
22 L. Xue, H. Gao, W. Zhou, S. Xin, K. Park, Y. Li and J. B. Goodenough, *Adv. Mater.*, 2016, **28**, 9608–9612.
23 D. Webster, *Metall. Trans. A*, 1987, **18**, 2181–2193.
24 E. Shpil'rain, V. Savchenko, A. G. Mozgovoi and S. N. Skovorod'ko, *High Temp.*, 2003, **41**, 23–31.
25 X. Guo, Y. Ding, L. Xue, L. Zhang, C. Zhang, J. B. Goodenough and G. Yu, *Adv. Funct. Mater.*, 2018, **28**, 1804649.
26 S. R. Reddy and J. P. Hajra, *CALPHAD: Comput. Coupling Phase Diagrams Thermochem.*, 1993, **17**, 151–156.
27 X. Feng and L. Jiang, *Adv. Mater.*, 2006, **18**, 3063–3078.
28 J. V. Naidich, *Progress in surface and membrane science*, Elsevier, 1981, vol. 14, pp. 353–484.
29 O. Dezellus and N. Eustathopoulos, *J. Mater. Sci.*, 2010, **45**, 4256–4264.
30 Z. Liang, D. Lin, J. Zhao, Z. Lu, Y. Liu, C. Liu, Y. Lu, H. Wang, K. Yan and X. Tao, *Proc. Natl. Acad. Sci. U. S. A.*, 2016, **113**, 2862–2867.
31 J. Wang, H. Wang, J. Xie, A. Yang, A. Pei, C.-L. Wu, F. Shi, Y. Liu, D. Lin, Y. Gong and Y. Cui, *Energy Storage Mater.*, 2018, **14**, 345–350.
32 X. Lu, G. Li, J. Y. Kim, D. Mei, J. P. Lemmon, V. L. Sprenkle and J. Liu, *Nat. Commun.*, 2014, **5**, 4578.
33 R. K. Kramer, J. W. Boley, H. A. Stone, J. C. Weaver and R. J. Wood, *Langmuir*, 2014, **30**, 533–539.
34 C. W. Wang, H. Xie, L. Zhang, Y. H. Gong, G. Pastel, J. Q. Dai, B. Y. Liu, E. D. Wachsman and L. B. Hu, *Adv. Energy Mater.*, 2018, **8**, 1701963.
35 X. Lu, M. E. Bowden, V. L. Sprenkle and J. Liu, *Adv. Mater.*, 2015, **27**, 5915–5922.
36 J. V. Naidich and J. N. Chuvashov, *J. Mater. Sci.*, 1983, **18**, 2071–2080.
37 L. Xue, W. Zhou, S. Xin, H. Gao, Y. Li, A. Zhou and J. B. Goodenough, *Angew. Chem., Int. Ed.*, 2018, **57**, 14184–14187.
38 L. Zhang, X. Xia, Y. Zhong, D. Xie, S. Liu, X. Wang and J. Tu, *Adv. Mater.*, 2018, **30**, 1804011.
39 L. Qin, W. Yang, W. Lv, L. Liu, Y. Lei, W. Yu, F. Kang, J.-K. Kim, D. Zhai and Q.-H. Yang, *Chem. Commun.*, 2018, **54**, 8032–8035.
40 L. Zhang, S. Peng, Y. Ding, X. Guo, Y. Qian, H. Celio, G. He and G. Yu, *Energy Environ. Sci.*, 2019, **12**, 1989–1998.
41 W. Luo, J. Wan, B. Ozdemir, W. Bao, Y. Chen, J. Dai, H. Lin, Y. Xu, F. Gu, V. Barone and L. Hu, *Nano Lett.*, 2015, **15**, 7671–7677.
42 L. Xue, H. Gao, Y. Li and J. B. Goodenough, *J. Am. Chem. Soc.*, 2018, **140**, 3292–3298.
43 Y. Ding, X. Guo, Y. Qian, L. Zhang, L. Xue, J. B. Goodenough and G. Yu, *Adv. Mater.*, 2019, **31**, 1806956.
44 X. B. Cheng, R. Zhang, C. Z. Zhao, F. Wei, J. G. Zhang and Q. Zhang, *Adv. Sci.*, 2016, **3**, 1500213.
45 E. J. Markvicka, M. D. Bartlett, X. Huang and C. Majidi, *Nat. Mater.*, 2018, **17**, 618–624.

 This journal is © The Royal Society of Chemistry 2019

Published on 28 June 2019. Downloaded by Fail Open on 7/23/2025 10:07:25 AM.

46 L. Hu, L. Wang, Y. Ding, S. Zhan and J. Liu, *Adv. Mater.*, 2016, **28**, 9210–9217.
47 R. D. Deshpande, J. C. Li, Y. T. Cheng and M. W. Verbrugge, *J. Electrochem. Soc.*, 2011, **158**, A845–A849.
48 Y. Wu, L. Huang, X. Huang, X. Guo, D. Liu, D. Zheng, X. Zhang, R. Ren, D. Qu and J. Chen, *Energy Environ. Sci.*, 2017, **10**, 1854–1861.
49 W. Yu, K. C. Lau, Y. Lei, R. Liu, L. Qin, W. Yang, B. Li, L. A. Curtiss, D. Zhai and F. Kang, *ACS Appl. Mater. Interfaces*, 2017, **9**, 31871–31878.
50 A. C. Baclig, G. McConohy, A. Poletayev, A. Michelson, N. Kong, J.-H. Lee, W. C. Chueh and J. Rugolo, *Joule*, 2018, **2**, 1287–1296.
51 L. Qin, W. Yang, W. Lv, L. Liu, Y. Lei, W. Yu, F. Kang, J. K. Kim, D. Zhai and Q. H. Yang, *Chem. Commun.*, 2018, **54**, 8032–8035.
52 C. Liu, X. Wang, W. Deng, C. Li, J. Chen, M. Xue, R. Li and F. Pan, *Angew. Chem., Int. Ed.*, 2018, **57**, 7046–7050.
53 C. Zhang, Y. Qian, Y. Ding, L. Zhang, X. Guo, Y. Zhao and G. Yu, *Angew. Chem., Int. Ed.*, 2019, **58**, 7045–7050.
54 C. Zhang, L. Zhang, Y. Ding, X. Guo and G. Yu, *ACS Energy Lett.*, 2018, **3**, 2875–2883.
55 Y. Ding, C. Zhang, L. Zhang, H. Wei, Y. Li and G. Yu, *ACS Energy Lett.*, 2018, **3**, 2641–2648.
56 C. Zhang, Z. Niu, S. Peng, Y. Ding, L. Zhang, X. Guo, Y. Zhao and G. Yu, *Adv. Mater.*, 2019, **31**, 1901052.
57 X. Zhou, Q. Liu, C. Jiang, B. Ji, X. Ji, Y. Tang and H. M. Cheng, *Angew. Chem., Int. Ed.*, 2019, DOI: 10.1002/anie.201814294.
58 S. H. Chen, J. Wang, L. Fan, R. F. Ma, E. J. Zhang, Q. Liu and B. G. Lu, *Adv. Energy Mater.*, 2018, **8**, 1800140.
59 L. Fan, K. Lin, J. Wang, R. Ma and B. Lu, *Adv. Mater.*, 2018, **30**, 1800804.
60 Y. Cheng, H. J. Chang, H. Dong, D. Choi, V. L. Sprenkle, J. Liu, Y. Yao and G. Li, *J. Mater. Res.*, 2016, **31**, 3125–3141.
61 T. Ichitsubo, S. Okamoto, T. Kawaguchi, Y. Kumagai, F. Oba, S. Yagi, N. Goto, T. Doi and E. Matsubara, *J. Mater. Chem. A*, 2015, **3**, 10188–10194.
62 J.-Z. Guo, Y. Yang, D.-S. Liu, X.-L. Wu, B.-H. Hou, W.-L. Pang, K.-C. Huang, J.-P. Zhang and Z.-M. Su, *Adv. Energy Mater.*, 2018, **8**, 1702504.
63 S. Zhang, B. Wang, J. Jiang, K. Wu, C. F. Guo and Z. Wu, *ACS Appl. Mater. Interfaces*, 2019, **11**, 7148–7156.
64 P. E. Mason, F. Uhlig, V. Vanek, T. Buttersack, S. Bauerecker and P. Jungwirth, *Nat. Chem.*, 2015, **7**, 250–254.